



# Use of shape memory alloy devices in heritage structures: application in San Silvestro belfry in L'Aquila

Ilaria Capanna<sup>a</sup> Franco Di Fabio<sup>a</sup>

<sup>a</sup> Department of Civil, Construction-Architectural and Environmental, University of L'Aquila, L'Aquila, 67100, Italy

*Keywords: Masonry culturale heritage; Shape memory alloy devices; seismic restoration; earthquake damage*

## ABSTRACT

Masonry cultural heritage structures exhibit a high brittleness when they are subjected to earthquake actions up to compromise their integrity. The Italian contest is characterized by a high seismic risk and vulnerability of the built heritage. In fact, many damages and collapses happened after seismic events causing the loss of structural portion of artistic interest and economic disbursements for rehabilitation. The survey of masonry cultural buildings damages highlights the partial inefficacy or insufficiency of traditional restoration through failure and collapse. The resort to innovative reinforcement techniques avoids aforementioned issue with more performance materials. In the earthquake engineering field, the use of shape memory alloy devices takes place. These devices are realized by unique alloys that display powerful characteristics, including high damping behaviour, super-elasticity and shape memory effect.

The percentage change of components (Nickel and Titanium) and thermo-mechanical treatment allow to modify the stiffness of the devices and consequently the transmitted force to connected structures.

The use of shape memory alloy devices ensures the improvement of structural performance, in static and dynamic conditions. At the same time, these devices respect reversibility, durability and compatibility criteria. The main advantage is the possibility to calibrate the devices constitutive behaviour in terms of stiffness, elastic and yielding displacement as needed.

However the calibration of the constitutive behaviour is the main planning difficulty which is worsened by the lack of Normative Code and tested design procedures. Until now, in Italy, few restorations with shape memory alloy devices are carried out. Below, pilota design for cultural heritage structures are mentioned: belfry of the S. Giorgio Church in Trignano, S.Serafino Church in Foligno, S.Francis Church in Assisi.

In this work, an analytic procedure is presented to characterize the constitutive behaviour of devices. Aiming at discussing the application of devices in cultural heritage, a numerical model is performed for a proposed restoration by the authors.

The structural reinforcement for earthquake retrofit of bell-tower of S.Silvestro Church is carried out, heavily damaged by the main-shock of 6th April 2009 and its aftershocks.

The use of shape memory alloy devices is finalized to improve the masonry flexural resistance with pre-stress postponing plastic behaviour and to increase the dissipation of the seismic energy by devices damping.

This paper wants to highlight the powerful advantages of restoration with the powerful devices in the masonry structures.

## 1 INTRODUCTION

### 1.1 Shape Memory Alloy Material

Shape Memory Alloys (SMAs) are performing materials due to the super-elasticity, the large ductility, corrosion and fatigue resistance and high damping characteristics.

These useful properties have introduced SMAs to several fields as biomedical, aerospace and engineering. SMAs are recently being used in earthquake applications to modify the seismic

structural response. In the last century, various shape memory alloys have been discovered.

In 1932, gold-cadmium was the first of the shape memory transformation.

In 1962, Buechler et al. discovered the Shape Memory Effect (SME) in nickel-titanium. (Song et al. 2006).

Nowadays the industry offers various SMA types: MnCu-based, FeMn[Si]-based, CuAlNi-based, NiTi-based. The Nickel and Titanium system is based on the equiatomic compound of Nickel and

Titanium. Ni-Ti SMAs seem to be the most appropriate to use in civil applications.

### 1.2 The Shape Memory Alloy Properties

SMAs exhibit the property to endure reversible phase transition processes changing crystallographic structure. The two crystal phase transformations in SMAs are austenite and martensite.

The austenite phase is stable at lower stress and higher temperature. It has a body-centered cubic crystal structure. The austenite phase has a unique orientation of the crystal structure so it exhibits high resistance to external stress.

The martensite phase is stable at higher stress and lower temperature. It has a parallelogram structure (orthorhombic) changing in 24 configurations. The compatible arrangement of the structure is allowed under the maximum elongation (self-accomodation).

The transition from austenite to martensite and the reverse transition are due to a thermal cycle.

The transition temperatures that characterize the thermal cycle are: austenite start temperature  $A_s$ , austenite finish temperature  $A_f$ , martensite start temperature  $M_s$  and martensite finish temperature  $M_f$ , (fig.1c).

At the macroscopic level, this phenomenon affects two characteristics: the shape memory effect (SME) and super-elasticity.

The SME allows the possibility to return back to original shape upon heating.

The super elasticity is related to the possibility to undergo large inelastic deformations and recover the shape after unloading.

### 1.3 The shape memory alloy effect

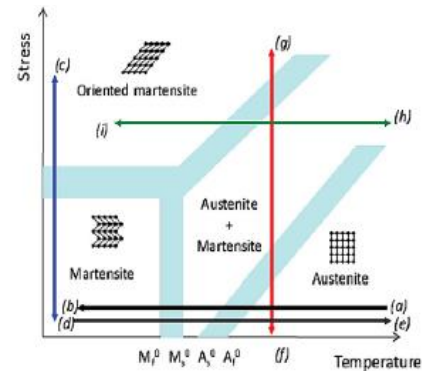
The detwinning process of martensitic variants occurs beyond a critical value applying a unidirectional stress to a martensitic specimen.

This phenomenon causes the spatial re-orientation of the martensitic variants in single-variant martensite characterized by detwinned structure. During the aforementioned process, the stress is constant until the martensite is totally detwinned with the aligned single variant along the stress direction. Straining the specimen, the elastic deformation takes place up to yielding in which the stress is constant. During unloading, the plastic deformation remains. Martensite changes in austenite by heating above  $A_f$  and the specimen recovers the original shape. This

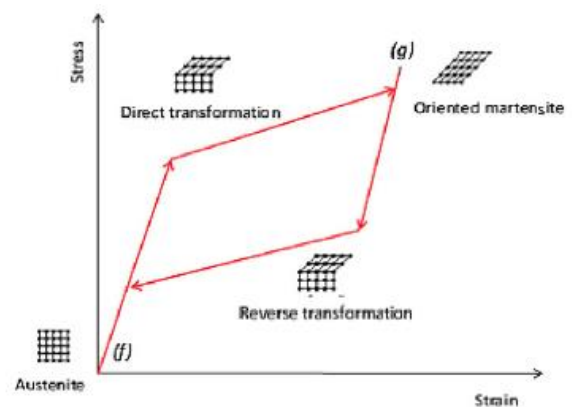
phenomenon is called Shape Memory Effect (SME).

### 1.4 The Shape Memory Alloy Super-Elasticity

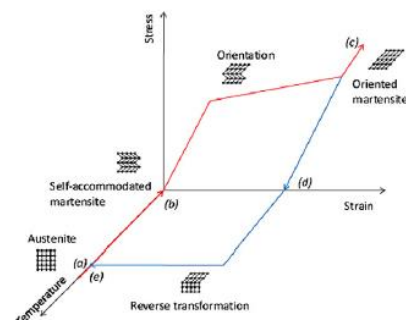
A transformation from austenite to detwinned martensite takes place beyond a critical value of temperature greater than  $A_f$  applying a unidirectional stress to a austenitic specimen.



a. schematic phase diagram for a SMA



b. pseudo elastic behaviour



c. One-way shape memory effect

Figure 1(a-b-c)- Illustration of typical phase diagram and key behaviours for SMAs (Morin et al. 2011).

During the transformation in isothermal conditions, the stress is constant until the material is totally transformed. Further straining causes the elastic loading of the detwinned martensite.

Immediately unloading, a reverse transformation occurs at a lower stress value, since martensite is weak without stress at temperature greater than  $A_f$ . This step causes an energy absorption capacity with zero residual strain. This phenomenon is called Super elasticity. In the figure 1, the representation of SMA behaviour is reported.

### 1.5 Shape Memory Alloy Devices

The powerful behaviour of SMAs allows a widespread use in civil engineering applications (figure 2). Different Shape Memory Alloy Devices (SMADs) are available with different shapes (wires and bars), geometric features (diameter and length), and physical properties as alloy composition, thermo-mechanical treatment, material phase (Dolce et al. 2001).

#### 1.5.1 Application to Masonry Cultural Heritage structures

Starting from the observation of Masonry Cultural Heritage structures (MCUHES) damages, it is possible to state that bad seismic behaviour was also caused by recent restoration measures that induced an enhancement of structural mass and stiffness. This issue is guiding towards a new interpretation of the restoration which pays attention to safety of architectural value (intrinsic artistic value and additional value due to frescos, buttresses and various architectural decorations) and to insurance of seismic protection.

The restoration of MCUHES with SMADs is advantageous, not only for seismic performance improvement, but because the insertion of the devices is external to the structure and totally reversible.

In this paper, the application of the SMADs is analyzed for slender structures that have high damping capacity due to the high vibration period. In particular structural situations, the large displacements cause hammering with adjacent constructions or local collapse of the masonry.

The application of SMADs to slender structure avoids the aforementioned issues. The stiffness of SMADs produces a re-centering force restoring the initial structural position. The damping of SMADs insures the dissipation of earthquake energy reducing the displacements of the structure (Parulekar et al. 2012).



Figure 2- Shaking table test of SMADs (FIP Industriale)

## 2 THE PROPOSED ANALYTIC METHOD TO DEFINE SMADS PARAMETERS

The lack of references in literature and Guidelines make the design of SMADs a difficult procedure. Moreover, in Italy, few realizations of restoration with SMADs are carried out: S.Serafino Church in Foligno, S.Francis Church in Assisi and belfry of the S. Giorgio Church in Trignano (Indirli et al. 2008).

In this paper, a proposed analytic method is developed in order to define the mechanic parameters of the devices: stiffness  $k_{SMADs}$  in the initial branch, in loading branch, the elastic and final displacements and the damping value  $c_{SMADs}$ .

A non linear kinematic method is proposed to assign stiffness and displacements of SMADs.

Whereas a modified Housner formulation is developed to evaluate the damping of SMADs (Housner 1963). Afterwards, a numerical model is performed in order to evaluate the real influence over seismic performance. The application to S.Silvestro belfry is the performed case study.

### 2.1 The non linear kinematic approach

The wall is considered as a rigid block that oscillates about the centre of rotation O (figure 3). The coefficient of friction is sufficiently large therefore sliding is absent between the rigid block and the base. The significant properties of the wall are its weight  $W$ , its moment of inertia  $I_0$ , about the point O, and the location of the centre of gravity at distance  $h$  above the base and  $l$  from the side. The shape memory alloy device is included in the kinematic model as a non linear vertical spring that generates a restoring force. The considered properties of the SMADs are the

restoring force  $F_{SMADs}$  and the application point of the spring A.

As shown in fig.3, the radial distance between the centre of rotation O and the centre of gravity is  $OG=(h^2+l^2)^{1/2}$ .

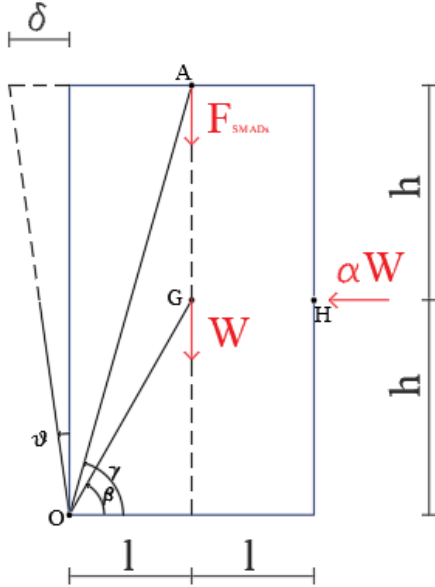


Figure 3- The wall rocking according to non linear kinematic approach

The distance between the centre of rotation O and the point A is equal to  $OA=(2h^2+l^2)^{1/2}$ .

When the block is at rest, the line OG makes an angle  $\beta$  and the line OA makes an angle  $\gamma$  with the horizontal. The tilting of the block from the vertical is measured by the angle  $\psi$ .

When the block is rotated through an angle  $\psi$ , the horizontal force  $\alpha W$  in the point H, proportional to the weight W in terms of a constant, generates an overturning moment  $M_{s,o}$  about the point O.

Whereas the restoring moment  $M_{R,O}$  are exerted by the weight and the restoring force of the device.

During the overturning, the rotation causes an infinitesimal variation of the distance between the application point of the forces and the pole O, as represented in figure 4. Therefore the position variations of the points A, G and H, are included in the equilibrium moment in terms of the horizontal component  $\partial x_i$  and the vertical component  $\partial y_i$ .

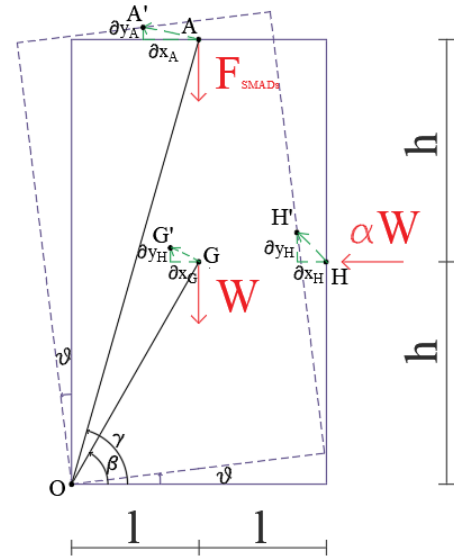


Figure 4- The configuration of the wall during the overturning

The equation of the moment equilibrium is reported in the equation 1:

$$\sum M_{S,O} = \sum M_{R,O} \quad (1)$$

$$\begin{aligned} \sum M_{S,O} &= W \cdot (l - \partial x_G) + F_{SMAD} \cdot (l - \partial x_A) \rightarrow \\ \sum M_{S,O} &= W \cdot (l - \partial x_G) + k_{SMAD} \cdot \partial y_A (l - \partial x_A) \end{aligned} \quad (2)$$

$$\sum M_{R,O} = \alpha \cdot W \cdot (h + \partial y_G) \quad (3)$$

In equation 2,  $k_{SMADs}$  is the stiffness of the spring,  $\partial x_G$  is the horizontal component of the displacement of the point G and  $\partial x_A$  is the horizontal component of the displacement of the point A.

In equation 3,  $\alpha$  is the constant for the horizontal loads,  $\partial y_G$  is the vertical component of the displacement of the point G.

Writing the equations 2 and 3 in terms of the rotation angle  $\psi$ :

$$\begin{aligned} W[l - OG \cdot (\cos \beta - \cos(\beta + \theta))] + \\ k_{SMADs} \cdot (OA \cdot (\sin(\gamma + \theta) - \sin \alpha)) \cdot \\ OA \cdot (\cos \gamma - \cos(\gamma + \theta)) = \\ \alpha \cdot W \cdot (h + R \cdot (\sin(\beta + \theta) - \sin \beta)) \end{aligned} \quad (4)$$

Imposing the maximum displacement (elastic and plastic)  $\delta$  at the top of the wall, the unknown variables of the shape memory alloy device are



obtained. At first, the stiffness of the device might be high in order to contribute to reduce the rocking of the wall (minor displacement and elastic state of masonry). Afterwards, the stiffness might be minor to employ the displacement capacity in order to dissipate the earthquake energy (greater displacement and plastic state of masonry). The maximum displacement at the top of the wall is established evaluating the flexural resistance moment at the bottom of the wall.

## 2.2 The Proposed Housner Formulation

The remaining unknown parameter of the shape memory alloy device is the damping value  $c_{SMADs}$ . The proposed approach is the Housner model in order to describe the rocking. The wall is considered as a rigid block that oscillates again through an angle  $\vartheta$ . For small angle  $\vartheta$  of oscillation, the effect of the acceleration is the same as of a horizontal force  $H$  acting through the gravity centre  $G$  of the wall.

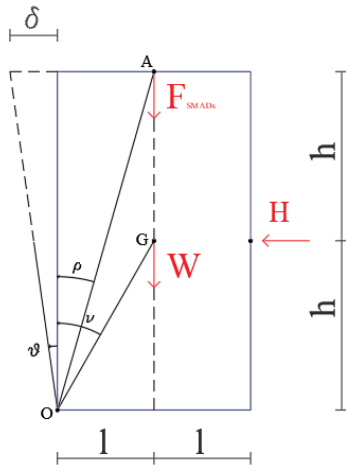


Figure 5- The rocking wall according Housner formulation

When the block is at rest, the line  $OG$  makes an angle  $\nu$  and the line  $OA$  makes an angle  $\rho$  with the vertical direction. The tilting of the block from the vertical is measured by the angle  $\vartheta$  (figure 5).

The equation of motion is written considering the rotation  $\vartheta$  as Lagrangian coordinate in the equation 5:

$$I_0 \frac{d^2\theta}{dt^2} + W \cdot OG \cdot \sin(\nu - \theta) + F_{SMADs} \cdot OA \cdot \sin(\rho - \theta) + c_{SMADs} \cdot \frac{d\theta}{dt} = H \cdot \cos\theta \quad (5)$$

Moreover for slender walls, the sine and the cosine of the angle may be approximated by the angle and the unitary value.

$$I_0 \frac{d^2\theta}{dt^2} - W \cdot OG \cdot \theta + c_{SMADs} \frac{d\theta}{dt} + W \cdot OG \cdot \nu - F_{SMADs} \cdot OA \cdot \theta + F_{SMADs} \cdot OA \cdot \rho = \frac{W \cdot OA \cdot \alpha}{g} \quad (6)$$

Setting  $W \cdot OA / I_0 = p^2$  in the equation 6, the equation becomes:

$$\frac{d^2\theta}{dt^2} - p^2 \cdot \nu + c_{SMADs} \cdot \frac{1}{I_0} \frac{d\theta}{dt} - F_{SMADs} \cdot \frac{OA}{I_0} \cdot \theta + F_{SMADs} \cdot \frac{OA}{I_0} \cdot \rho = \frac{p^2 \cdot \alpha}{g} \quad (7)$$

Performing a non linear dynamic analysis, the trend of displacement is evaluated. The max displacement in a specific instant of the time might be imposed to avoid hammering or local collapse.

Imposing the max value of displacement and the corresponding time in the equation 7, the only unknown parameter is  $c_{SMADs}$ . The solution of the dynamic equation gives the damping coefficient concluding the characterization of the devices.

## 3 THE APPLICATION OF SMADS TO S.SILVESTRO BELFRY

Aiming at evaluating the efficacy of the application of SMADs to MCUHES, numerical analysis are carried out. The chosen case study is the belfry of S.Silvestro church that is located in the centre of L'Aquila (the related data were available from Ministry of Cultural Heritage Department).

It is a typical medieval church with symmetric facade and the bell-tower was added in the 19th century. After the 2009 earthquake, the tower reported heavy cracks due to two different overturning mechanisms (figure 6, Ministry of Cultural Heritage) which can be identified by visible cracking pattern from right side wall.

The first mechanism is defined by a diagonal crack starting from the bottom wall to the facade corona. The second mechanism involves the upper part of the belfry and it is also defined by a diagonal crack. The first diagonal crack goes from the base of the bell-cell to the church roof, the second crack restarts from the latter position to the base of bell cell. The two mechanisms created a cylindrical hinge in correspondence of the connection between tower and external wall of the lateral aisle causing the crack and the expulsion of the cantonal stone blocks.



Figure 6- The two mechanisms of overturning

The damage scenario is more serious in two points due to concentrated tensions: at the base of the belfry (due to compression hinge) and at the height church eaves (10.20 meters, due to hammering).

### 3.1 Structural Model

After the 6<sup>th</sup> April earthquake, the local authorities carried out a diagnostic campaign in order to assess the cultural building restoration. The absence of wall-to-wall connections was proved by the results of the diagnostic campaign (figure 7, Ministry of Cultural Heritage). Therefore the modelling of single walls of the belfry is a realistic choice. The selected wall for the analysis is the lateral wall. Non destructive tests have been carried out in order to characterize the masonry. Endoscopic tests were performed at different heights. The found data are scattered and inhomogeneous. The investigated masonry is a rubble material with regular stones embedded in thick mortar. The constitutive law, employed in the model of masonry, is quasi-brittle in tension and elasto-plastic in compression. The mechanical properties of the masonry are reported in the table 1.

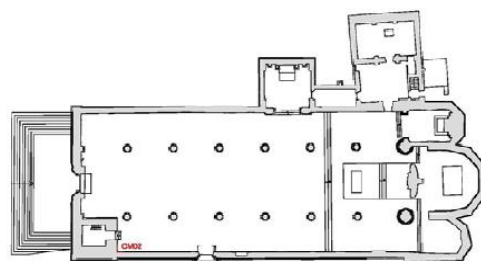


Figure 7-Report of diagnostic campaigns

Table 1. Mechanical properties of masonry

Compressive strength $f_m$	Shear resistance $\tau$	Elastic modulus E	Shear modulus G	$\gamma$
(N/mm <sup>2</sup> )	(N/mm <sup>2</sup> )	(N/mm <sup>2</sup> )	(N/mm <sup>2</sup> )	(kN/m <sup>3</sup> )
320	0.065	1740	580	21

The structural model is implemented in a finite element software. The description of the model is reported in the table 2. Square shell with non linear material are employed in the model. The restraint at the base of the wall is modelled by springs reacting compression only.

Table 2. Characteristics of the Finite Element model

E.F. MODEL FEATURES	
E.F. type	Square shell
masonry wall length	4.8 m
masonry wall height	21.6 m
height of the belfry	28.8 m
thickness	1.00 m
number of E.F.	371
number of nodes	240
analysis plane	xz

The assessment of devices effectiveness over the structure is carried out by non-linear static analysis, linear dynamic analysis and non-linear dynamic analysis history.

Push over analysis were performed following the recommendations of the Ministerial Decree (D.M.2018). Seismic loads are represented by uniform pattern of lateral loads proportional both

to mass and to first vibration mode of the structure. The results of push-over analysis proportional to mass are reported.

Time-history analysis were performed assigning natural records and the solution of the motion equation was obtained by direct integration method.

### 3.2 Seismic response ante restoration

In the current state, before the proposed restoration, the seismic performance of the structure is restricted due to the high tensile stress. Analyzing the stress distribution, a compression stress state is concentrated at the base of the wall and near the large windows due to re-distribution of tensional flow, whereas a widespread tensile state is located in the masonry spandrel owing to the low value of gravity loads. In the figure 8, push over curve is reported.

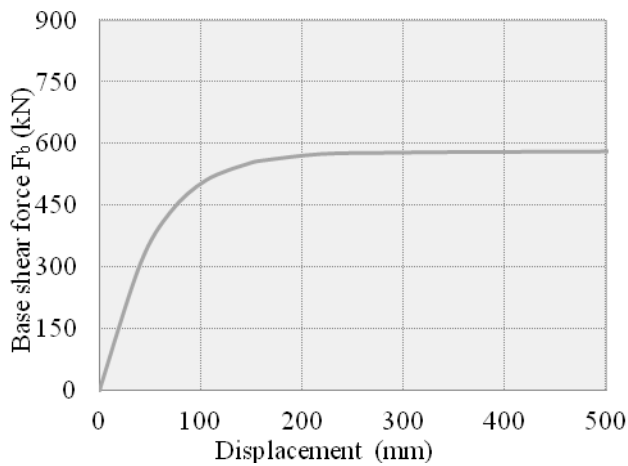


Figure 8- Push over curve ante restoration

The base shear force  $F_b$  of the wall achieves the value of 586 kN.

### 3.3 Seismic Response After The Application Of Bars And SMADs

The main goals of the proposed restoration are the enhancement of masonry flexural resistance and the generation of restoring force imposed on the masonry wall during the earthquake.

The restoration measure consists of the application of steel profile located in series with SMADs directed along the vertical direction, as represented in figure 9.

The bars are pre-tensioned by a tensile force of 150 kN transferring a pre-compression stress to masonry. The pre-compression of material increases the flexural resistance contrasting the tensile stress that arise during earthquake motion.

The two tie bars, formed by three segments to facilitate their assembly ( $\phi 30$ , S355), are fixed at steel laminate profiles that are installed on the top and the bottom of the wall section. Steel laminate profiles contribute to spread the stress evenly. The increase of compression tensional state due to pre-compression ranges up to the maximum value of  $35 \text{ N/cm}^2$ . The four SMADs are installed in series with bars.

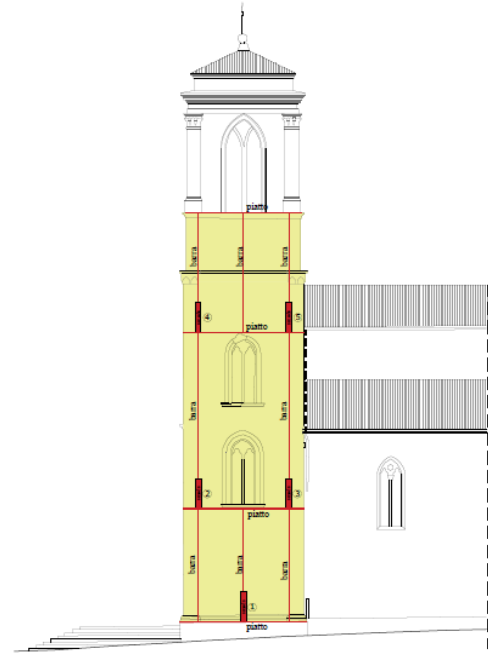


Figure 9- Proposal restoration in S.Silvestro belfry

#### 3.3.1 The Assessment Of Seismic Response

Firstly, the role of the devices is to generate a restoring force. Their law-behaviour is calibrated on the max permissible displacement for the structure in order to avoid hammering with adjacent constructions or local collapse.

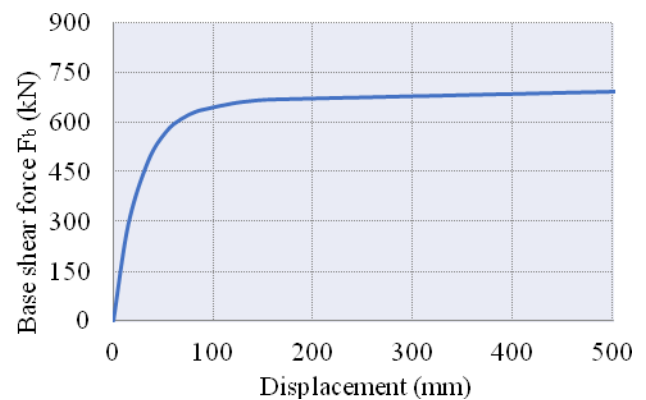


Figure 10-Push over curve after steel bars application

Non linear static analysis is repeated after the application of pre-tensioned bars (the curve push-over is reported in figure 10) and after the

installation of SMADs (the curve push-over is reported in figure 11). The push-over curve in figure 10 shows the benefit of the pre-compression by steel bars compared to the ante-restoration seismic response. After that, the application of SMADs increases the seismic performance due to the restoring force (figure 11). In fact, higher deformations of the structures produce higher deformations of the devices and consequently major restoring forces.

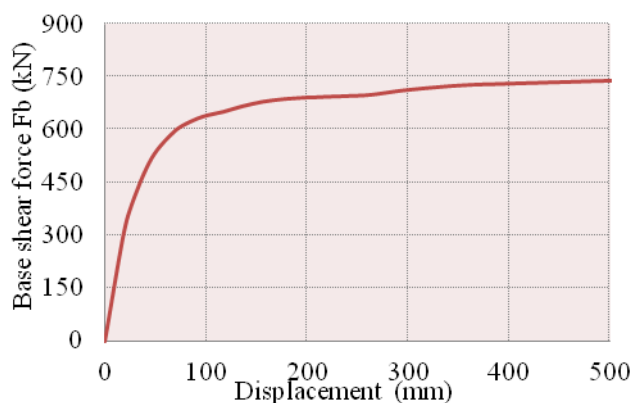


Figure 11- Push over curve after steel bars application

The trend of the deformation in the SMADs is reported in the following figure (figure 12)

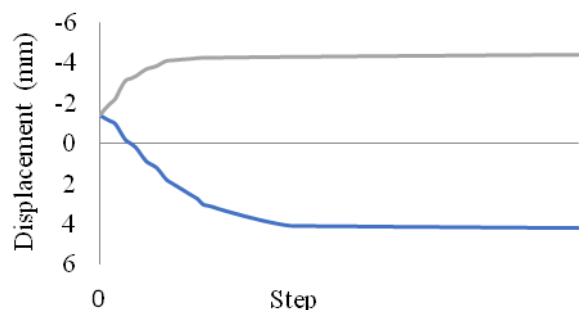


Figure 12- Deformation in n° 2 and 3

Therefore the restoring forces balance the deformation of the structure during the horizontal seismic action improving the seismic response.

### 3.4 The assessment of the displacement control

Dynamic analysis are performed in order to evaluate the influence of SMADs on the structure displacement.

The result of the modal analysis highlights that the first vibration mode has the similar trend between the ante-restoration case and the post-restoration case, as shown in figure 13. The devices leave unchanged the modal shape: although the stiffness of the structure increases,

the stiffness variation is uniform along the height of the belfry.

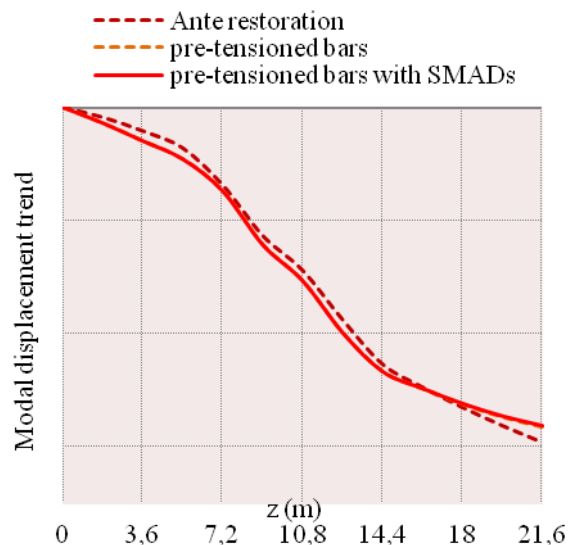


Figure 13- The first modal mode along the height of belfry

In order to evaluate the damping of the SMADs, the displacements history of the belfry is investigated by a time history analysis. The 3 adopted accelerograms, for the non linear dynamic analyses, were selected in the strong motion record database extrapolated from Rexel v3.5 (Iervolino et al. 2009) being compatible spectrum with the target code response spectrum. Below, the 3 records are described in the table 3. The analyzed case is the most unfavourable, for the structural response, that was obtained assigning the second record to the belfry. The monitored node is at the base of bell-cell. The integration of motion equation is performed up to 10 seconds.

Name	ID	Date	Distance [km]	M <sub>w</sub>
1 L'Aquila Mainshock	AQK	6/4/09	56.50	6.3
2 Friuli 4 <sup>th</sup> shock	FRC	15/9/76	168.3	5.9
3 L'Aquila Mainshock	AQV	6/04/09	8.78	6.3

The displacements in the case of the wall with SMADs are minor than in the case ante-restoration (figure 14).



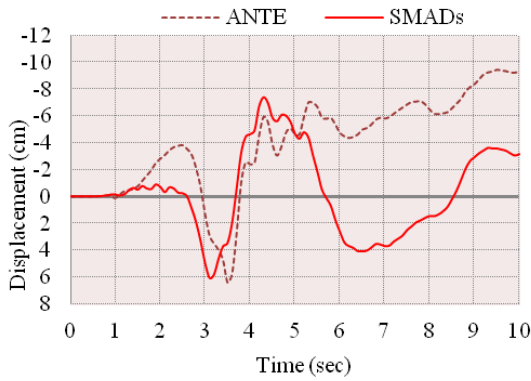


Figure 14- Displacement in the time domain

Initially, the trend of displacements is similar between the case ante restoration and the case post restoration. Nevertheless, from 5 second, the decrease of the numerical displacement value occurs allowing the control of plasticization state of the masonry.

The ultimate displacement in the SMADs case is minor than ante-restoration case avoiding hammering phenomenon. This result puts in evidence the effectiveness of SMADs working that controls the rocking of the belfry and the overcoming of admissible displacements.

#### 4 CONSIDERATIONS AND DISCUSSIONS

The innovative restoration with SMADs is compared with traditional restoration, as the application of binding mixtures. The conventional measures (cracked masonry global consolidations, re-plastering, use of polymeric materials) increase the mechanical properties of masonry proportionally to a constant coefficient. A traditional restoration with binding mixtures is applied to the masonry wall modifying the mechanical properties with the coefficient 1.5 (in accord to Italian Guidelines n.7/2009).

The comparison of push-over curves of different restorations is reported in figure 15:

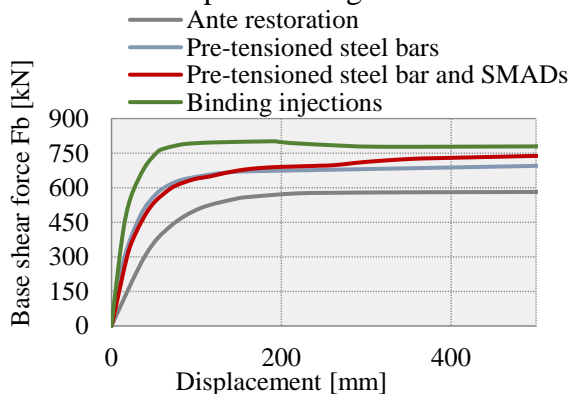


Figure 15- Comparison of push-over curves

As figure 15 shows, the initial branch of the conventional restoration curve is more tilted than the others because the elastic modulus of the masonry increases changing the dynamic structural property. According to the dynamic modal results, also the initial branch of the restoration with SMADs curve is more tilted than the ante restoration case. On the other hand, the stiffness growth, due to these devices, is less noticeable than other cases.

In non linear field, the value of the base shear force is similar between the traditional restoration and innovative restoration. This result underlines the effectiveness of SMADs in order to improve the seismic performance of the structure.

Also the conventional restoration improves the seismic response but it is invasive.

The retrofit with SMADs ensures a satisfactory behaviour of the belfry due to the enhancement of the seismic capacity in terms of force and displacements. The restoring forces preserve the equilibrium of the structure. The stiffness and damping of the shape memory alloy devices monitor the displacements trend in order to avoid hammering phenomena.

The advantages of SMADs are not only reinforcement and retrofit of MCUHES but also feasibility to resolve structural issue.

In fact, the properties of the devices could be calibrated on slender structures which are characterized by variations of stiffness and acceleration amplification along the height protecting precious structural parts.

#### REFERENCES

- Dolce, M., Cardone, D., 2001. Mechanical behaviour of shape memory alloys for seismic applications: Austenite NiTi wires subjected to tension. *International Journal of Mechanical Sciences*, **43**, 2657-2677
- Morin, C., Moumni, Z., Zaki, W., 2011. A constitutive model for shape memory alloys accounting for thermomechanical coupling. *International Journal of Plasticity*, **27**, 748-767
- Song, G., Ma, N., N.Li, H., 2006. Applications of shape memory alloys in civil structures. *Engineering structures*, **28**, 1266-1274
- Parulekar, Y.M., Reddy, G.R., Vaze, K.K., Guha, S., Gupta, C., Muthumani, K., Sreekala, R., 2012. Seismic response attenuation of structures using shape memory alloy dampers. *Structural control and health monitoring*, **19**, 102-119
- Indirli, M., Castellano, M.G., 2008. Shape Memory Alloy Devices for the Structural Improvement of Masonry Heritage Structures. *International Journal of Architectural Heritage*, **2:2**, 93-119

- Housner, W.G., 1963. The behaviour of inverted pendulum structures during earthquakes. *Bulletin of the Seismological Society of America*, **2**, 403-417
- Ministry for Cultural Heritage and Activities. Guidelines for evaluation and mitigation of seismic risk to cultural heritage.
- Cisse, C., Zaki, W., Ben Zineb, T., 2016. A review of constitutive models and modelling techniques for shape memory alloys. *International Journal of Plasticity*, **76**, 244-284
- Ministro delle Infrastrutture, 2018. Aggiornamento Norme Tecniche per le costruzioni (NTC18).
- Ministro delle Infrastrutture, 2019. Istruzioni per l'applicazione delle nuove Norme Tecniche per le costruzioni (Circolare n.7 del 21 Gennaio 2019).
- Iervolino, I., Galasso, C., Cosenza, E., 2009. Rexel: computer aided record selection for code-based seismic structural analysis. *Bulletin of Earthquake Engineering*, **8**, 339-363.
- Ministro delle Infrastrutture, 2019. Istruzioni per l'applicazione delle nuove Norme Tecniche per le costruzioni (Circolare n.7 del 21 Gennaio 2019).